ISSN 1392-1207. MECHANIKA. Vol. 29, No. 3, 2023: 252–257

Influence of Geometrical Shape on the Lubrication Performance of Partially Micro-Grooved Gas-Lubricated Parallel Slider Bearings

Fuxi LIU*, Chunjie YANG, Shanwu XU***, Kang XIE****, Dunzhao XIE*****, Binhui HAN******, Zhanlong LI*******

**School of Mechanical and Electrical Engineering, Hunan Applied Technology University, Changde 415100, China, E-mail: liufx28@163.com*

***College of Automation, Xi'an University of Posts and Telecommunications, Xi'an 710121, China, E-mail: 13772188915@163.com*

****School of Mechanical and Electrical Engineering, Hunan Applied Technology University, Changde 415100, China, E-mail: 2876495246@qq.com*

*****School of Mechanical and Electrical Engineering, Hunan Applied Technology University, Changde 415100, China, China, E-mail: 857706372@qq.com*

******School of Mechanical and Electrical Engineering, Hunan Applied Technology University, Changde 415100, China, E-mail: 2723548754@qq.com*

*******School of Automotive Engineering, Xi'an Aeronautical Polytechnic Institute, Xi'an 710089, China, E-mail: hbhzayy@126.com*

********School of Mechanical Engineering, Taiyuan University of Science and Technology, Taiyuan 030024, China, E-mail: lizl@tyust.edu.cn (Corresponding author)*

https://doi.org/10.5755/j02.mech.32384

1. Introduction

Opening micro-grooves has been applied to enhance the mechanical component performance for many years [1-3]. Recently, researchers study the performance of micro-grooved mechanical components using an incompressible lubricant. Adatepe et al. [4] experimentally and numerically studied the tribological performance of micro-grooved oil-lubricated journal bearings. They found that the experimental results are in accordance with the numerical results. Kango et al. [5] theoretically investigated the friction coefficient of micro-grooved oil-lubricated journal bearings. It was shown that micro-grooves could decrease the friction coefficient. Kumar et al. [6] studied the frictional power loss of micro-grooved thrust bearings using an incompressible lubricant. They showed that the frictional power loss could be reduced by opening micro-grooves. Fu et al. [7] studied the lubrication performance of fully micro-grooved oil-lubricated parallel slider bearings. It was found that the hydrodynamic pressure could be increased by using the optimized micro-groove geometrical parameters. Ji et al. [8] studied the influence of grooving parameters and micro-groove cross-section shape on the lubrication performance of partially micro-grooved oil-lubricated parallel slider bearings. Their results demonstrated that grooving parameters and micro-groove cross-section shape have a significant impact on the lubrication performance of partially micro-grooved fluid-lubricated parallel slider bearings. Miao et al. [9] investigated the tribological performance of micro-grooved oil-lubricated piston ring-cylinder liner components. It was shown that micro-grooves could produce better tribological performance at proper conditions.

Researchers also investigate micro-grooved mechanical components using a compressible lubricant. Yan et al. [10] investigated the performance of micro-grooved gas-lubricated foil journal bearings. It was found that opening micro-grooves on the top foil could increase the pressure around the load domain and decrease the end leakage. By using the chaos-enhanced accelerated particle swarm algorithm, Yu et al. [11] studied the performance of micro-grooved gas-lubricated thrust bearings. It was found that the discontinuous micro-grooves could obtain the higher load-carrying capacity. Kou et al. [12] investigated the steady and dynamic performances of micro-grooved gas seals at high-speed conditions. Their results showed that the super ellipse grooves could produce the larger state-film stiffness and dynamic stiffness coefficients. Lu et al. [13] investigated the influence of geometrical parameters of micro-grooves on the lubrication performance of fully micro-grooved gas-lubricated parallel slider bearings. They found that the average pressure of fully micro-grooved gas-lubricated parallel slider bearings is controlled by the geometrical parameters of micro-grooves.

The influence of grooving parameters and micro-groove cross-section shape on the lubrication performance of partially micro-grooved oil-lubricated parallel slider bearings has been systematically investigated [8]. However, the influence of grooving parameters and micro-groove cross-section shape on the lubrication performance of partially micro-grooved gas-lubricated parallel slider bearings is not investigated. The present study is intended to study the influence of grooving parameters and micro-groove cross-section shape on the lubrication performance of partially micro-grooved gas-lubricated parallel slider bearings. Firstly, the model of partially micro-grooved gas-lubricated parallel slider bearings is established. Secondly, the multi-grid finite element method is adopted to solve the dimensionless compressible Reynolds equation for the steady-state form. Finally, the influences of the orientation angle of the micro-grooves, the depth of the micro-grooves, the width of the micro-grooves, the area density of the micro-grooves, and micro-grooved fraction on average pressure are investigated for different micro-groove cross-section shapes.

2. The model

Fig. 1 presents the model of partially micro-grooved gas-lubricated parallel slider bearings. *x* axel is parallel to the sliding direction of the lower slider and *y* axel is perpendicular to the sliding direction of the lower slider. The lower slider and upper slider are separated by the gas and the speed of the lower slider is *U*. The gas between the lower slider and upper slider is a Newtonian fluid and the gas flow between the lower slider and upper slider is isothermal and laminar. The upper slider is fixed and the micro-grooves are evenly distributed in the upper slider. The minimum gas film thickness of partially micro-grooved gas-lubricated parallel slider bearings is *c*. The length of the micro-grooved zone is l_m and the depth of each micro-groove is h_g.

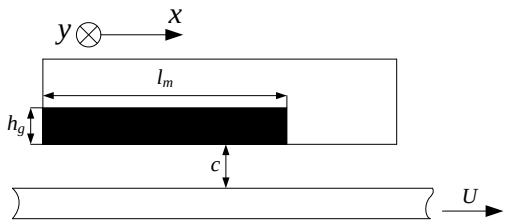

Fig. 1 Model of partially micro-grooved gas-lubricated parallel slider bearings [8, 14]

Fig. 2 presents the model of the partially micro-grooved slider. *O* is the origin of the coordinate system. The length of the partially micro-grooved slider is *l*. The micro-groove orientation angle is θ and the micro-groove spacing is s_g. The width of each micro-groove is w_g. In Fig. 2, b, the cross-section shape of the micro-groove along the *A-A* direction is rectangle. In Fig. 2, c, the cross-section shape of the micro-groove along the *A-A* direction is triangle. In Fig. 2, d, the cross-section shape of the micro-groove along the *A-A* direction is parabola.

The micro-groove area density s_p is defined as:

$$s_p = \frac{w_g}{w_g + s_g}. \tag{1}$$

The micro-grooved fraction f_m is defined as:

$$f_m = \frac{l_m}{l}. \tag{2}$$

The compressible Reynolds equation for the steady-state form is described as [13]:

$$\frac{\partial}{\partial x}\left(ph^3\frac{\partial p}{\partial x}\right)+\frac{\partial}{\partial y}\left(ph^3\frac{\partial p}{\partial y}\right)=6\mu U\frac{\partial(ph)}{\partial x}, \tag{3}$$

where: *h* is the thickness of the gas film; *p* is the pressure; μ is the viscosity.

The dimensionless variables are defined as:

$$X = x/w_0,\ \ Y = y/w_0,\ \ P = p/p_a,\ \ H = h/c, \tag{4}$$

where: w_0 is the reference value; p_a is the ambient pressure.

The dimensionless compressible Reynolds equation for the steady-state form is given by:

$$\frac{\partial}{\partial X}\left(PH^3\frac{\partial P}{\partial X}\right)+\frac{\partial}{\partial Y}\left(PH^3\frac{\partial P}{\partial Y}\right)=\Lambda\frac{\partial(PH)}{\partial X}, \tag{5}$$

where: $\Lambda = 6\mu U w_0/(p_a c^2)$.

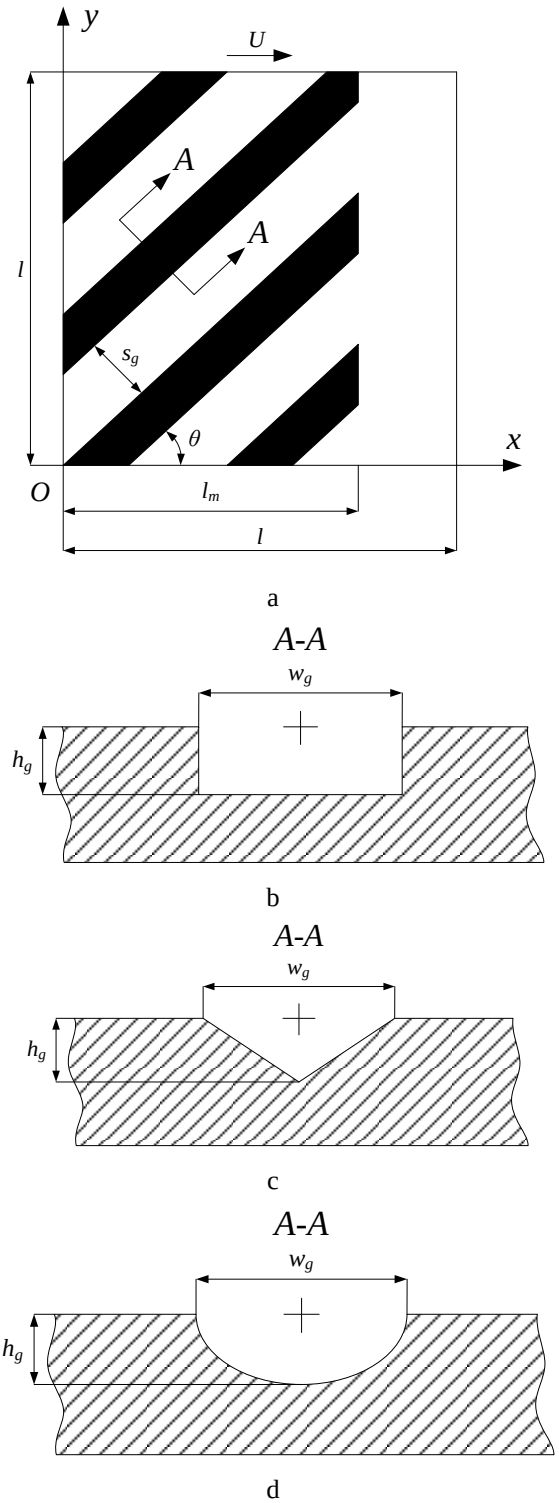

Fig. 2 Geometric model of the partially micro-grooved slider [8]: a) distribution of the micro-grooves; b) cross-section shape of the rectangular groove; c) cross-section shape of the triangular groove; d) cross-section shape of the parabolic groove

The dimensionless thickness *H* is given by:

case 1: $0° \le \theta < 90°$ for the rectangular grooves in Fig. 2, b:

$$H(X,Y)=\begin{cases}1+H_g \\ \quad Y<Xtan\theta, Y_1<Y<Y_2, \text{and } X\le f_mL \\ 1+H_g \\ \quad Y>Xtan\theta, Y_3<Y<Y_4, \text{and } X\le f_mL \\ 1, \quad \text{elsewhere}\end{cases}, \tag{6}$$

for the triangular grooves in Fig. 2, c:

$$H(X,Y)=\begin{cases}1+\dfrac{2H_g}{W_g}\left(\dfrac{1}{2}W_g-\left|Xsin\theta-Ycos\theta-\left(n_1L_g-\dfrac{1}{2}W_g\right)\right|\right) \\ \quad Y<Xtan\theta, Y_1<Y<Y_2, \text{and } X\le f_mL \\ 1+\dfrac{2H_g}{W_g}\left(\dfrac{1}{2}W_g-\left|Ycos\theta-Xsin\theta-\left(n_1L_g-S_g-\dfrac{1}{2}W_g\right)\right|\right) \\ \quad Y>Xtan\theta, Y_3<Y<Y_4, \text{and } X\le f_mL \\ 1, \quad \text{elsewhere}\end{cases}, \tag{7}$$

for the parabolic grooves in Fig. 2, d:

$$H(X,Y)=\begin{cases}1+H_g-\dfrac{4H_g}{W_g^2}\left(Xsin\theta-Ycos\theta-\left(n_1L_g-\dfrac{1}{2}W_g\right)\right)^2 \\ \quad Y<Xtan\theta, Y_1<Y<Y_2, \text{and } X\le f_mL \\ 1+H_g-\dfrac{4H_g}{W_g^2}\left(Ycos\theta-Xsin\theta-\left(n_1L_g-S_g-\dfrac{1}{2}W_g\right)\right)^2 \\ \quad Y>Xtan\theta, Y_3<Y<Y_4, \text{and } X\le f_mL \\ 1, \quad \text{elsewhere}\end{cases}, \tag{8}$$

case 2: $\theta = 90°$for the rectangular grooves in Fig. 2, b:

$$H(X,Y)=\begin{cases}1+H_g \\ \quad X>n_2L_g, X<n_2L_g+W_g, \text{and } X\le f_mL \\ 1, \quad \text{elsewhere}\end{cases}, \tag{9}$$

for the triangular grooves in Fig. 2, c:

$$H(X,Y)=\begin{cases}1+\dfrac{2H_g}{W_g}\left(\dfrac{1}{2}W_g-\left|X-n_2L_g-\dfrac{1}{2}W_g\right|\right) \\ \quad X>n_2L_g, X<n_2L_g+W_g, \text{and } X\le f_mL \\ 1, \quad \text{elsewhere}\end{cases}, \tag{10}$$

for the parabolic grooves in Fig. 2, d:

$$H(X,Y)=\begin{cases}1+H_g-\dfrac{4H_g}{W_g^2}\left(X-n_2L_g-\dfrac{1}{2}W_g\right)^2 \\ \quad X>n_2L_g, X<n_2L_g+W_g, \text{and } X\le f_mL \\ 1, \quad \text{elsewhere}\end{cases}, \tag{11}$$

where:

$$\left.\begin{aligned}Y_1&=Xtan\theta-(n_1L_g+W_g)sec\theta \\ Y_2&=Xtan\theta-n_1L_g\sec\theta \\ Y_3&=Xtan\theta+(n_1L_g+S_g)sec\theta \\ Y_4&=Xtan\theta+(n_1+1)L_gsec\theta\end{aligned}\right\}, \tag{12}$$

$$L_g=(w_g+s_g)/w_0, \tag{13}$$

$$n_1=fix\left|(Xsin\theta-Ycos\theta)/L_g\right|, \tag{14}$$

$$n_2=fix\left|X/L_g\right|, \tag{15}$$

where: *fix* is a function returning a value towards the nearest integer; $S_g = s_g/w_0$ is the dimensionless micro-groove spacing; $W_g = w_g/w_0$ is the dimensionless micro-groove width; $H_g = h_g/c$ is the dimensionless micro-groove depth; $L = l/w_0$ is the dimensionless length of the partially micro-grooved slider.

The boundary condition of Eq. (5) is described as:

$$P(0,Y)=P(L,Y)=P(X,0)=P(X,L)=1. \tag{16}$$

The multi-grid finite element method [14] is adopted to solve Eq. (5) and the dimensionless pressure P is obtained. The dimensionless average pressure P_{av} is calculated by:

$$P_{av}=\frac{p_{av}}{p_a}=\frac{\int_0^L\int_0^L PdXdY}{L^2}. \tag{17}$$

3. Results and discussions

When the effect of grooving parameters and micro-groove cross-section shape on the hydrodynamic lubrication performance of partially micro-grooved gas-lubricated parallel slider bearings is investigated, some calculation parameters are constant. The constant are as follows: $\mu = 1.8 \times 10^{-5}$ Pa·s; $l = 2.5$ mm; $w_0 = 0.05$ mm; $c = 3 \times 10^{-4}$ mm; $p_a = 0.101325$ MPa; $U = 4$ m/s. In this study, the program is executed by using Matlab software.

The dimensionless pressure distributions for the parabolic grooves, rectangular grooves, and triangular grooves are shown in Fig. 3. It is observed that the pressure behaviors of the three micro-groove cross-section shapes are very similar and the maximum pressures can be found at the right side of the micro-grooved zone. It is also observed that the maximum pressure generated by the rectan-

gular grooves is obviously greater than those generated by the parabolic grooves and triangular grooves.

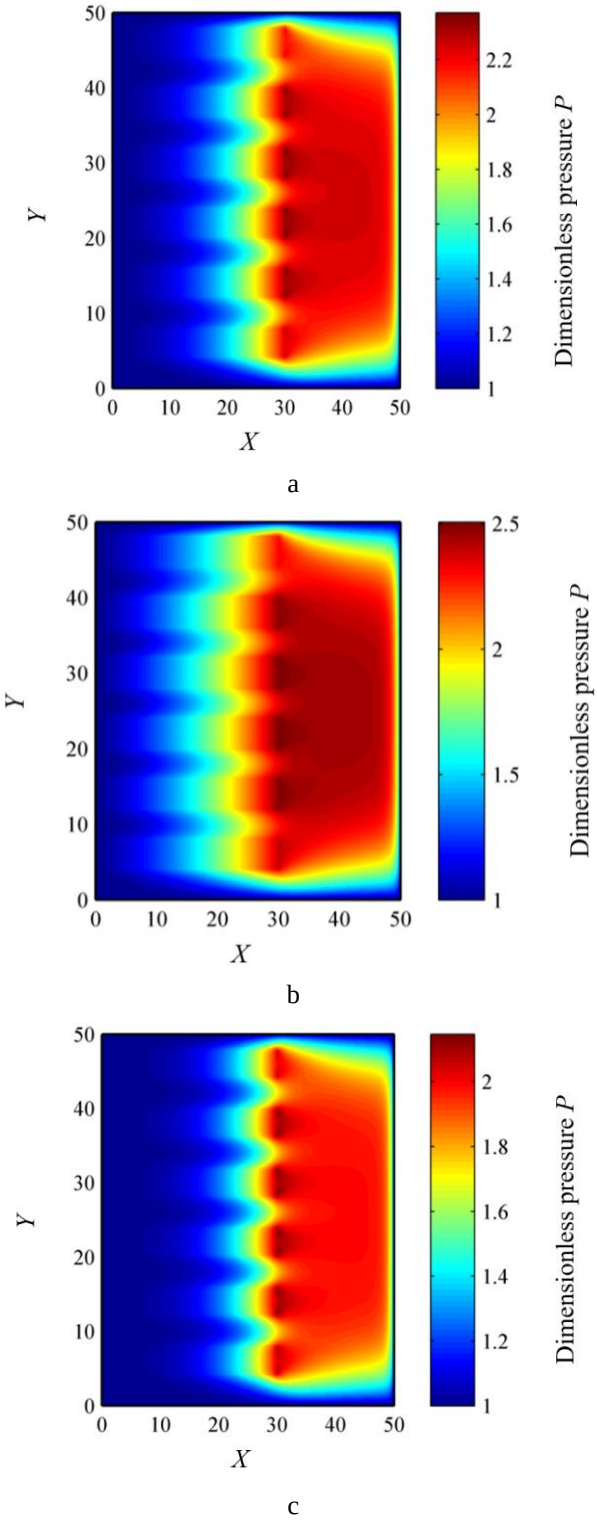

Fig. 3 Dimensionless pressure distributions for: a) the parabolic grooves; b) the rectangular grooves; c) the triangular grooves (θ = 0°; H_g = 4; W_g = 4; s_p = 0.5; f_m = 0.6)

Fig. 4 shows the influence of the orientation angle of the micro-grooves on average pressure for different micro-groove cross-section shapes. It is noted that the micro-grooves parallel to the sliding direction generate the maximum average pressure. The result is in accordance with that obtained by Ji et al. [8]. It is also noted that the maximum average pressure generated by the rectangular grooves is greater than those generated by the parabolic grooves and the triangular grooves. The result differs from that obtained by Ji et al. [8]. This is due to the fact that Ji et al. [8] employ an incompressible lubricant and the present study employs a compressible lubricant.

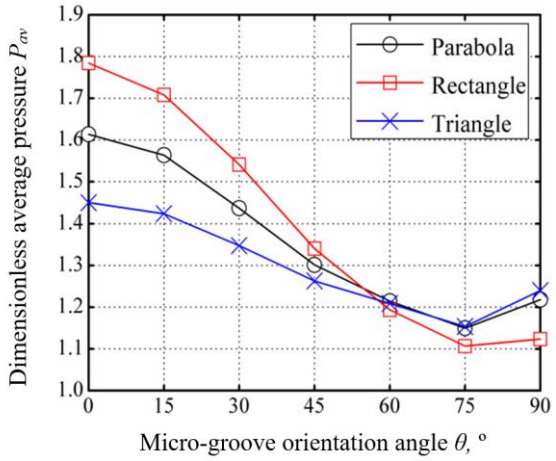

Fig. 4 Influence of the orientation angle of the micro-grooves on average pressure for different micro-groove cross-section shapes (H_g = 4; W_g = 4; s_p = = 0.5; f_m = 0.6)

Fig. 5 presents the influence of the depth of the micro-grooves on average pressure for different micro-groove cross-section shapes. With increasing the depth of the micro-grooves, the average pressure first increases, then reaches a maximum value, and finally decreases. It shows that there is an optimum micro-groove depth to maximize the average pressure. Furthermore, the optimum micro-groove depth is dependent on the micro-groove cross-section shape. These results are in accordance with those obtained by Ji et al. [8].

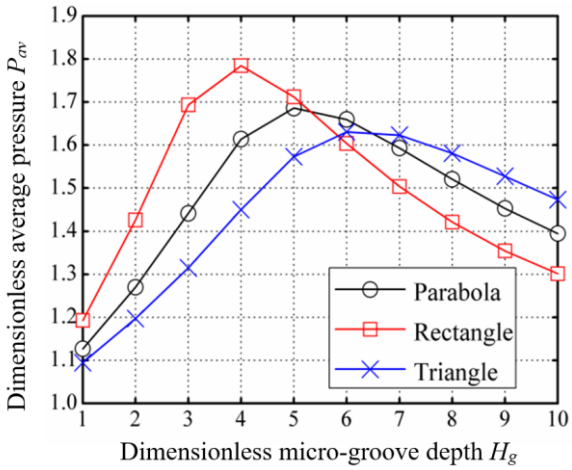

Fig. 5 Influence of the depth of the micro-grooves on average pressure for different micro-groove cross-section shapes (θ = 0°; W_g = 4; s_p = 0.5; f_m = 0.6)

Fig. 6 shows the influence of the width of the micro-grooves on average pressure for different micro-groove cross-section shapes. The results indicate that there is an optimum micro-groove width to maximize the average pressure. The results also indicate that the optimum micro-groove width is dependent on the micro-groove cross-section shape. The result differs from that obtained by Ji et al. [8].

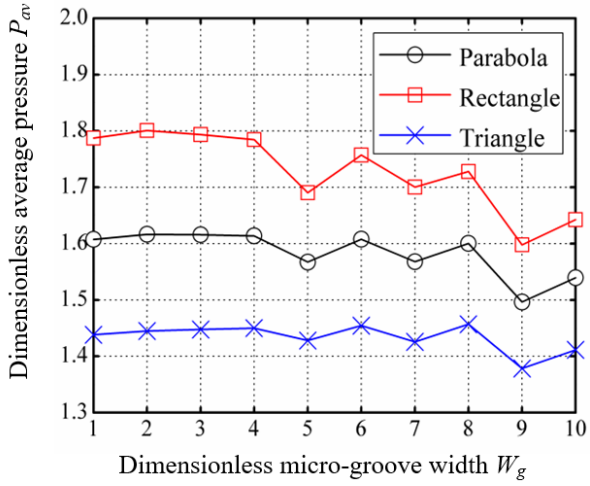

Fig. 6 Influence of the width of the micro-grooves on average pressure for different micro-groove cross-section shapes (θ = 0°; H_g = 4; s_p = 0.5; f_m = 0.6)

Fig. 7 presents the influence of the area density of the micro-grooves on average pressure for different micro-groove cross-section shapes. The average pressure increases with increasing the area density of the micro-grooves. For this reason, the area density of the micro-grooves should be chosen as large as possible for maximizing the average pressure. Furthermore, the maximum average pressure generated by the rectangular grooves is greater than those generated by the parabolic grooves and the triangular grooves. These results are in accordance with those obtained by Ji et al. [8].

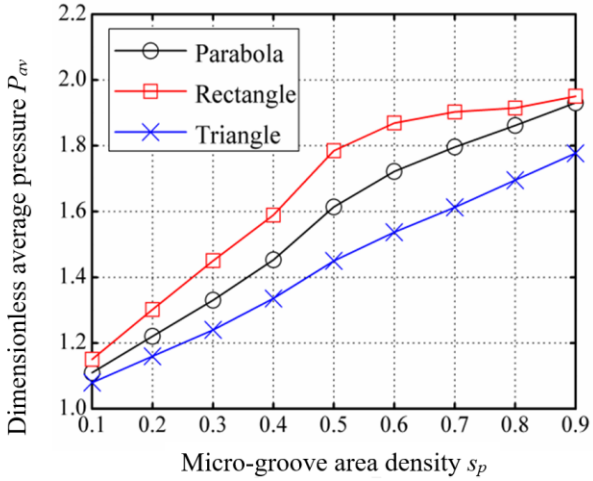

Fig. 7 Influence of the area density of the micro-grooves on average pressure for different micro-groove cross-section shapes (θ = 0°; H_g = 4; W_g = 4; f_m = = 0.6)

Fig. 8 presents the influence of micro-grooved fraction on average pressure for different micro-groove cross-section shapes. With the increase of micro-grooved fraction, the average pressure first increases, then reaches a maximum value, and finally decreases. It shows that there is an optimum micro-grooved fraction to maximize the average pressure. Furthermore, the optimum micro-grooved fraction is dependent on the micro-groove cross-section shape. These results are in accordance with those obtained by Ji et al. [8].

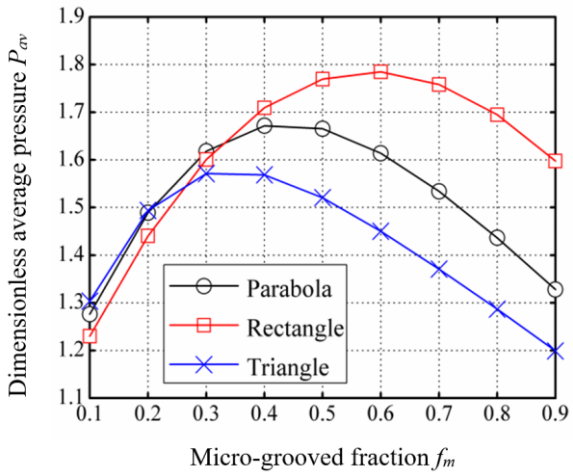

Fig. 8 Influence of micro-grooved fraction on average pressure for different micro-groove cross-section shapes (θ = 0°; H_g = 4; W_g = 4; s_p = 0.5)

4. Conclusions

A hydrodynamic lubrication model of partially micro-grooved gas-lubricated parallel slider bearings is established to investigate the influence of grooving parameters and micro-groove cross-section shapes on the lubrication performance of partially micro-grooved gas-lubricated parallel slider bearings. The grooving parameters include orientation angle of the micro-grooves, depth of the micro-grooves, width of the micro-grooves, area density of the micro-grooves, and micro-grooved fraction. The micro-groove cross-section shape includes parabola, rectangle, and triangle. The average pressure is chosen as the valuation criteria, and the influence of grooving parameters on average pressure is analyzed for different micro-groove cross-section shapes. The following conclusions are obtained:

1. The micro-grooves parallel to the sliding direction could generate the maximum average pressure. However, the influence of micro-groove cross-section shapes on the maximum average pressure is different. The maximum average pressure generated by the rectangular grooves is greater than those generated by the parabolic grooves and the triangular grooves.

2. The optimum micro-groove depth for maximizing the average pressure, the optimum micro-groove width for maximizing the average pressure, and the optimum micro-grooved fraction for maximizing the average pressure are dependent on the micro-groove cross-section shape.

3. The average pressure increases with the increase of micro-groove area density. Therefore, the area density of the micro-grooves should be chosen as large as possible for obtaining the maximum average pressure. However, the influence of micro-groove cross-section shapes on the maximum average pressure is different. The maximum average pressure generated by the rectangular grooves is greater than those generated by the parabolic grooves and the triangular grooves.

Acknowledgments

This study is supported by the Doctor Startup Project of Hunan Applied Technology University under Grant No. 2021HYBS04.

References

1. **Kumada, Y.; Hashizume, K.; Kimura, Y.** 1996. Performance of plain bearings with circumferential microgrooves, Tribology Transactions 39(1): 81-86. http://dx.doi.org/10.1080/10402009608983505.
2. **Yu, T. H.; Sadeghi, F.** 2001. Groove effects on thrust washer lubrication, Journal of Tribology 123(2): 295-304. http://dx.doi.org/10.1115/1.1308014.
3. **Suh, M. S.; Chae, Y. H.; Kim, S. S.; Hinoki, T.; Kohyama, A.** 2010. Effect of geometrical parameters in micro-grooved crosshatch pattern under lubricated sliding friction, Tribology International 43(8): 1508-1517. http://dx.doi.org/10.1016/j.triboint.2010.02.012.
4. **Adatepe, H.; Bıyıklıoglu, A.; Sofuoglu, H.** 2013. An investigation of tribological behaviors of dynamically loaded non-grooved and micro-grooved journal bearings, Tribology International 58: 12-19. http://dx.doi.org/10.1016/j.triboint.2012.09.009.
5. **Kango, S.; Sharma, R. K.; Pandey, R. K.** 2014. Comparative analysis of textured and grooved hydrodynamic journal bearing, Journal of Engineering Tribology 228(1): 82-95. http://dx.doi.org/10.1177/1350650113499742.
6. **Kumar, V.; Sharma, S. C.; Narwat, K.** 2020. Influence of micro-groove attributes on frictional power loss and load-carrying capacity of hybrid thrust bearing, Industrial Lubrication and Tribology 72(5): 589-598. http://dx.doi.org/10.1108/ILT-07-2019-0278.
7. **Fu, Y. H.; Ji, J. H.; Bi, Q. S.** 2012. Hydrodynamic lubrication of conformal contacting surfaces with parabolic grooves, Journal of Tribology 134(1): 011701-1-9. http://dx.doi.org/10.1115/1.4005518.
8. **Ji, J. H.; Fu, Y. H.; Bi, Q. S.** 2014. Influence of geometric shapes on the hydrodynamic lubrication of a partially textured slider with micro-grooves, Journal of Tribology 136(4): 041702-1-8. http://dx.doi.org/10.1115/1.4027633.
9. **Miao, J. Z.; Li, Y. Q.; Rao, X.; Zhu, L. B.; Guo, Z. W.; Yuan, C. Q.** 2020. Effects of different surface grooved cylinder liner on the tribological performance for cylinder liner-piston ring components, Industrial Lubrication and Tribology 72(5): 581-588. http://dx.doi.org/10.1108/ILT-01-2019-0012.
10. **Yan, J. J.; Zhang, G. H.; Liu, Z. S.; Zhao, J. M.; Xu, L.** 2018. Performance of a novel foil journal bearing with surface micro-grooved top foil, Journal of Engineering Tribology 232(9): 1126-1139. http://dx.doi.org/10.1177/1350650117737210.
11. **Yu, Y. L.; Pu, G.; Jiang, T. C.; Jiang, K.** 2020. Discontinuous grooves in thrust air bearings designed with CAPSO algorithm, International Journal of Mechanical Sciences 165: 105197-1-9. http://dx.doi.org/10.1016/j.ijmecsci.2019.105197.
12. **Kou, G. Y.; Li, X. H.; Wang, Y.; Lin, M. Y.; Tan, C. S.; Mou, M. F.** 2020. Steady performance and dynamic characteristics of a superellipse groove dry gas seal at a high-speed condition, Industrial Lubrication and Tribology 72(6): 789-796. http://dx.doi.org/10.1108/ILT-05-2019-0171.
13. **Lu, Y. J.; Liu, F. X.; Zhang, Y. F.** 2017. Hydrodynamic lubrication of micro-grooved gas parallel slider bearings with parabolic grooves, Mechanika 23(6): 931-936. http://dx.doi.org/10.5755/j01.mech.23.6.19850.
14. **Liu, F. X.; Li, Z. L.; Yang, C. J.; Wu, H. B.; Yin, H. Z.; Jiang, S.** 2021. Hydrodynamic lubrication of partially textured gas parallel slider bearings with orientation ellipse dimples, Mathematical Problems in Engineering 2021: 1-7. http://dx.doi.org/10.1155/2021/4441892.

F. Liu, C. Yang, S. Xu, K. Xie, D. Xie, B. Han, Z. Li

INFLUENCE OF GEOMETRICAL SHAPE ON THE LUBRICATION PERFORMANCE OF PARTIALLY MICRO-GROOVED GAS-LUBRICATED PARALLEL SLIDER BEARINGS

S u m m a r y

The influence of grooving parameters and micro-groove cross-section shape on the lubrication performance of partially micro-grooved gas-lubricated parallel slider bearings is investigated in the present study. The solution procedure for the multi-grid finite element method is that the algebraic equations formed by the finite element method are in turn smoothed by the interpolation from the coarse grid to the fine grid and the restriction from the fine grid to the coarse grid. By adopting the multi-grid finite element method, the pressure distribution of partially micro-grooved gas-lubricated parallel slider bearings is obtained. The grooving parameters are optimized to obtain the maximum average pressure for different micro-groove cross-section shapes. The results show that the orientation angle of the micro-grooves, depth of the micro-grooves, width of the micro-grooves, area density of the micro-grooves, micro-grooved fraction, and cross-section shape of the micro-grooves have an important influence on the hydrodynamic pressure of partially micro-grooved gas-lubricated parallel slider bearings. The results of this study demonstrate that the lubrication performance of partially micro-grooved gas-lubricated parallel slider bearings can be obviously enhanced by adopting the appropriate grooving parameters and micro-groove cross-shape. The results of this study are beneficial for the design of partially micro-grooved gas-lubricated parallel slider bearings.

Keywords: gas-lubricated parallel slider bearings, micro-grooves, cross-section shape, lubrication performance.

Received September 21, 2022
Accepted June 14, 2023